Supplementary Information

Mussel-mimetic Thermal Conductive Films with Solid-solid Phase Change and Shape-adaptive Performance

Donglei Li[a], *Canxia Ding*[a], *Sicong Shen*[a], *Jun Wang*[a], *Limin Wu*[a], *Bo You*[a*] *Guibao Tao*[b*]

[a] Department of Materials Science and Advanced Coatings Research Center of Ministry of Education of China, Fudan University, Shanghai, 200438, People's Republic of China.

[b] State Key Laboratory of Mechanical Transmissions/ College of Mechanical and Vehicle Engineering, Chongqing University, Chongqing 400044, P. R. China

Corresponding Author

[*]E-mail: youbo@fudan.edu.cn (B. You), gbtao@cqu.edu.cn (G.B. Tao)

This file contains

S1. Supporting figures: Figure S1-S8

S2. Supporting tables: Table S1-S5

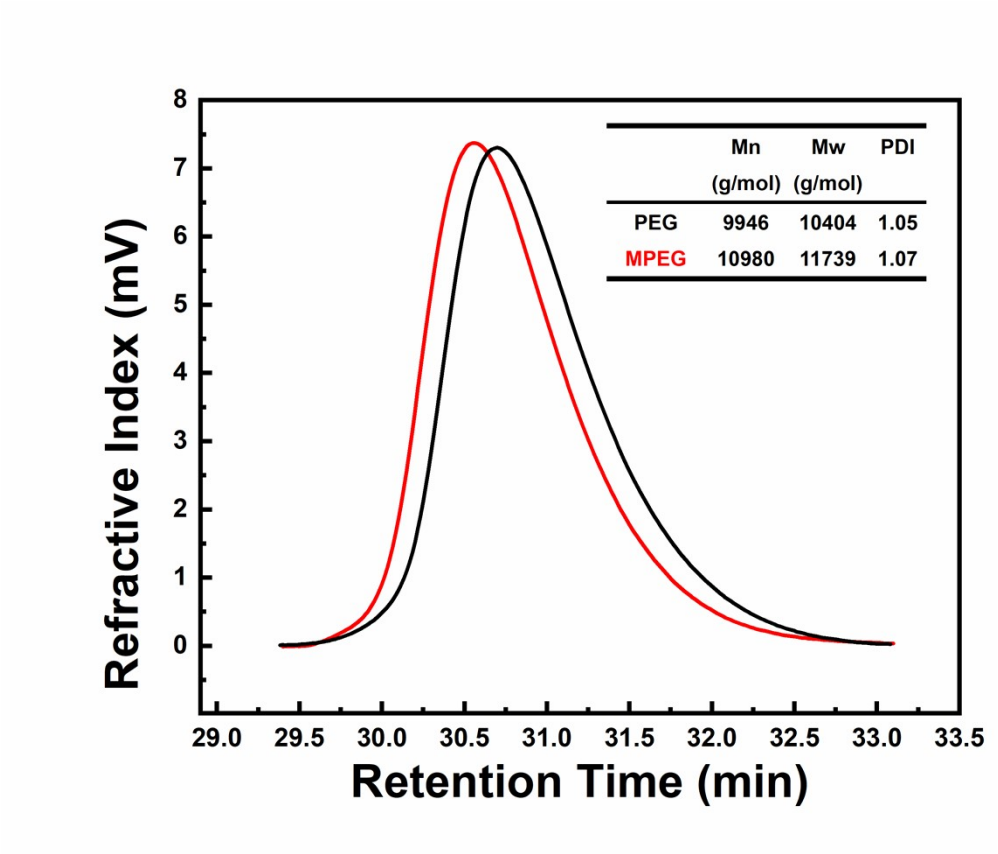

Figure S1. Gel permeation chromatography (GPC) of PEG and MPEG.

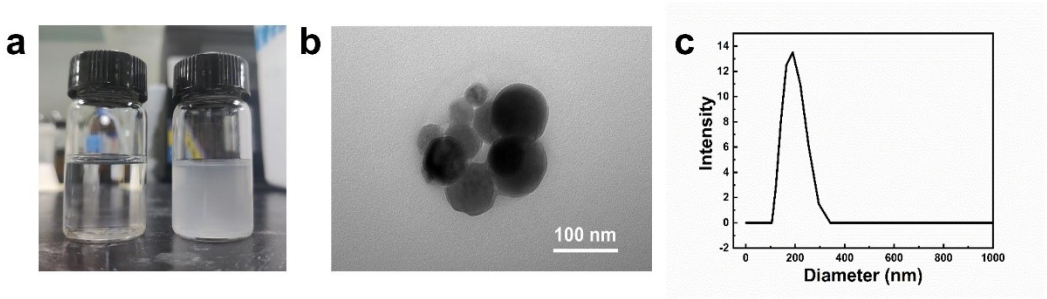

Figure S2. (a) Photos of PEG (left) and MPEG (right) aqueous solutions at 10 mg/mL. (b) High contrast transmission electron microscopy image of MPEG spherical aggregates in 10 mg/mL aqueous solution. (c) Particle size distribution of MPEG spherical aggregates in 10 mg/mL aqueous solution.

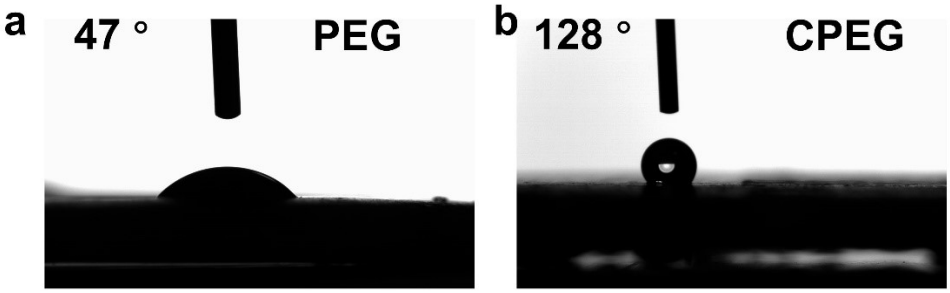

1

2 Figure S3. Water contact angle of (a) PEG film and (b) CPEG film.

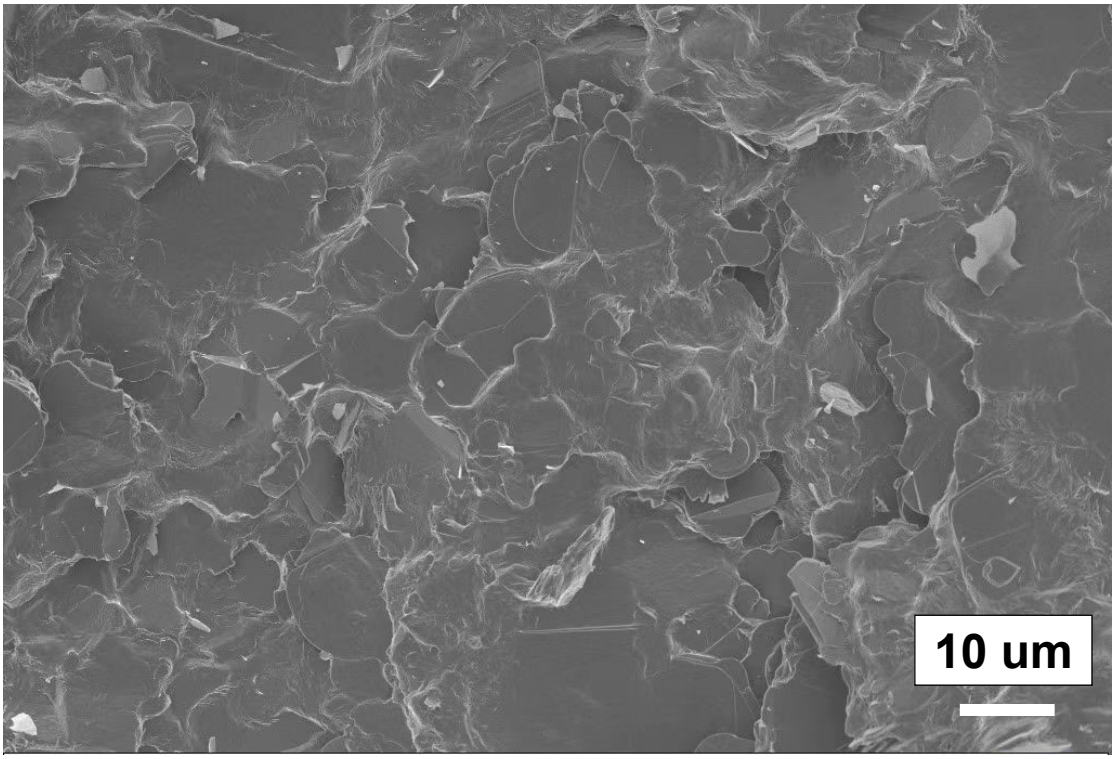

Figure S4. SEM image of the surface of bio-BN/CPEG film with 20vol% BN filling.

Figure S5. Photo of using an infrared thermal imager to test LED lamp bead temperature.

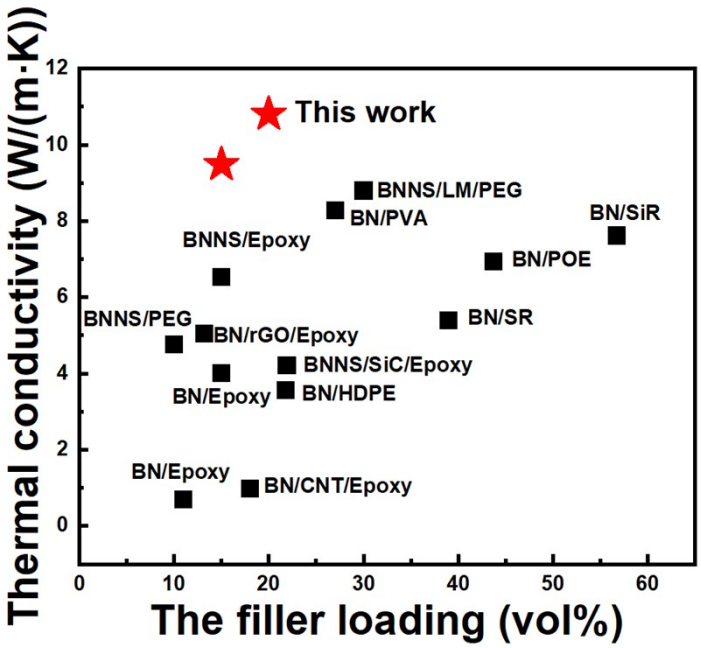

Figure S6. Comparison the maximum thermal conductivity of our film with the previously reported BN-based polymer composites under different BN loading loads.

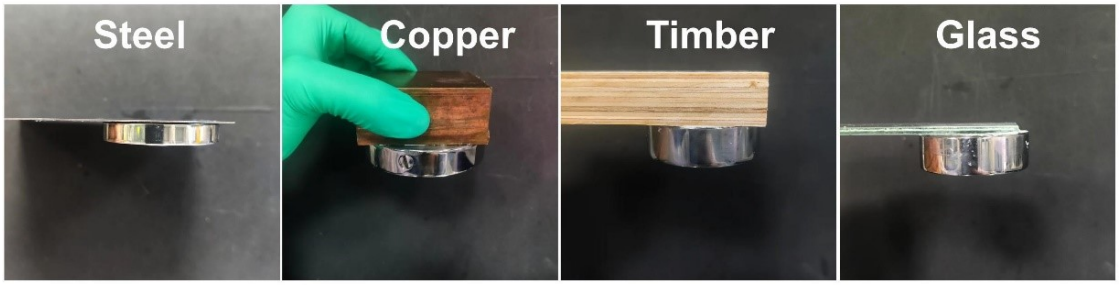

Figure S7. Demonstration of adhesion of bio-composite films with 20 vol% BN filler to different substrates at room temperature.

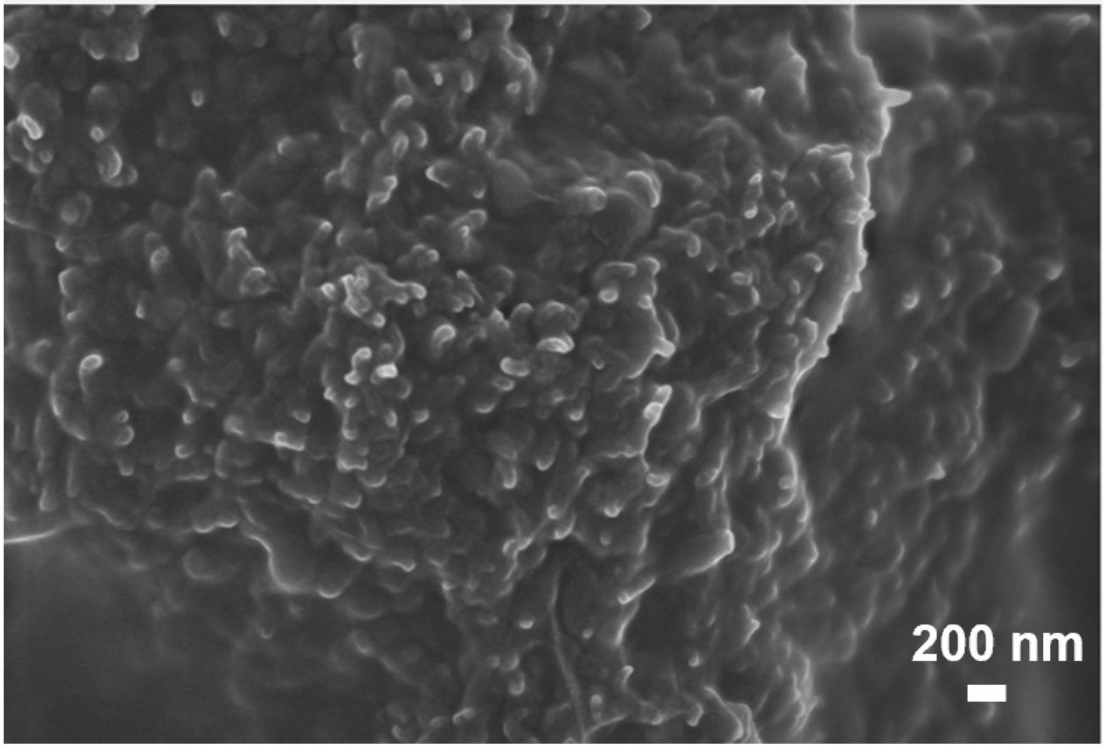

Figure S8 SEM images of MPEG aggregates in aqueous solution at high concentration (100 mg/mL).

Table S1 The difference of boron nitride content and preparation method in different samples.

Samples	The volume fraction of BN (%)	The mass fraction of BN (%)	Whether or not it has undergone a hot-pressing process
O-BN/CPEG-5	5	9	Yes
O-BN/CPEG-10	10	18	Yes
O-BN/CPEG-15	15	27	Yes
O-BN/CPEG-20	20	34	Yes
R-BN/CPEG-5	5	9	No
R-BN/CPEG-10	10	18	No
R-BN/CPEG-15	15	27	No
R-BN/CPEG-20	20	34	No

Table S2 DSC heating and cooling characteristics of the samples in the temperature range of -10-90 °C.

Sample	ΔH_h [J/g]	T_h [°C]	ΔH_C [J/g]	T_C [°C]
PEG	178	65.2	173	39.9
CPEG	155	59.8	151	43.2
O-BN/CPEG-5	141	59.8	141	43.4
O-BN/CPEG-10	124	59.1	120	44.0
O-BN/CPEG-15	111	59.3	107	43.1
O-BN/CPEG-20	103	59	101	43.5

Table S3 Comparison of the thermal conductivity of our O-BN/CPEG bio-composite film with previously reported results

Sample	$\lambda_{in\text{-}plane}$ [W/(m·K)]	$\lambda_{cross\text{-}plane}$ [W/(m·K)]	The filler loading (vol%)	Reference
This work	9.48	1.44	15	
This work	10.8	2.43	20	
BNNS/GO/PEG	4.41	2.55	11.65	[1]
BNNS/LM/PEG	8.8	7.64	30	[2]
BN/CNT/Epoxy	0.98	0.99	18	[3]
BNNS/Epoxy	6.54	0.7	15	[4]
BNNS/SiC/Epoxy	1.43	4.22	21.9	[5]
BNNS/PEG	4.76	1.29	10	[6]
BNNS/PDMS	11.05	1.15	10	[7]
BN/rGO/Epoxy	3.5	5.05	13.16	[8]
BN/HDPE	3.57	0.62	21.8	[9]
BN/PVA	8.28	0.63	27	[10]
BN/Epoxy	0.7	0.7	11	[11]
BN/POE	0.72	6.94	43.75	[12]
BN/SR	0.74	5.4	39	[13]
BN/SiR	1.3	7.62	56.7	[14]
BN/Epoxy	4.02	3.87	15	[15]

Table S4 Comparison of the thermal conductivity and latent heat of phase transition of our O-BN/CPEG bio-composite film with previously reported results for PEG-based phase change materials

Sample	Latent heat [J/g]	Thermal conductivity [W/(m · K)]	The filler loading (vol%)	Reference
This work	141	1.02	5	
This work	120	1.52	10	
This work	107	9.48	15	
This work	101	10.8	20	
BNNS/GO/PEG	147.5	4.41	11.65	[1]
BNMS/LM/PEG	80	8.8	30	[2]
CNTs/PEG	78.5	0.5	1.5	[16]
BN/CF/PEG	107.9	1.66	32	[17]
WG/HNT@AgNPs/PEG	103.6	1.15	25	[18]
CNT/PVP/PEG	103	0.265	4.1	[19]
BNNS/GO/PEG	121.9	2.62	10	[20]
BNNS/PEG	122.8	4.76	10	[6]
BNNS/GNP/PEG	116	1.33	17	[21]
BN/BC/PEG	134	3.26	16.3	[22]
BN/GO/PEG	131	2.36	12.5	[23]
BP/PEG	103	1.81	20	[24]

Table S5 Thermal diffusion coefficient, density, specific heat capacity and thermal conductivity of O-BN/CPEG bio-composite film with different hexagonal boron nitride micron content.

Sample	Thermal diffusion coefficient [mm^2/s]	Density [g/cm^3]	Specific heat capacity [J/ (g·K)]	Thermal conductivity [W/(m · K)]
CPEG (in-plane)	0.19	1.1	1.91	0.40
CPEG (out-of-plane)	0.12	1.1	1.91	0.25
O-BN/CPEG-5 (in-plane)	0.45	1.17	1.95	1.02
O-BN/CPEG-5 (out-of-plane)	0.18	1.17	1.95	0.41
O-BN/CPEG-10 (in-plane)	0.63	1.28	1.86	1.52
O-BN/CPEG-10 (out-of-plane)	0.30	1.28	1.86	0.72
O-BN/CPEG-15 (in-plane)	4.05	1.36	1.72	9.48
O-BN/CPEG-15 (out-of-plane)	0.62	1.36	1.72	1.44
O-BN/CPEG-20 (in-plane)	4.50	1.41	1.71	10.85
O-BN/CPEG-20 (out-of-plane)	1.01	1.41	1.71	2.44

Reference

1 D. Liu, C. Lei, K. Wu, *et al.*, A multidirectionally thermoconductive phase change material enables high and durable electricity via real-environment solar–thermal–electric conversion, *ACS Nano*, 2020, **14**(11), 15738-15747.

2 C. Guo, L. He, Y. Yao, *et al.*, Bifunctional liquid metals allow electrical insulating phase change materials to dual-mode thermal manage the li-ion batteries, *Nano-Micro Lett.*, 2022, **14**(1), 202.

3 Z. Su, H. Wang, J. He, *et al.*, Fabrication of thermal conductivity enhanced polymer composites by constructing an oriented three-dimensional staggered interconnected network of boron nitride platelets and carbon nanotubes, *ACS Appl. Mater. Interfaces*, 2018, **10**(42), 36342-36351.

4 J. Han, G. Du, W. Gao, *et al.*, An anisotropically high thermal conductive boron nitride/epoxy composite based on nacre-mimetic 3d network, *Adv. Funct. Mater.*, 2019, **29**(13), 1900412.

5 C. Xiao, Y. Guo, Y. Tang, *et al.*, Epoxy composite with significantly improved thermal conductivity by constructing a vertically aligned three-dimensional network of silicon carbide nanowires/ boron nitride nanosheets, *Compos. B. Eng.*, 2020, **187**, 107855.

6 C. Lei, K. Wu, L. Wu, *et al.*, Phase change material with anisotropically high thermal conductivity and excellent shape stability due to its robust cellulose/bnnss skeleton, *J. Mater. Chem. A*, 2019, **7**(33), 19364-19373.

7 H. Hong, Y. H. Jung, J. S. Lee, *et al.*, Anisotropic thermal conductive composite by the guided assembly of boron nitride nanosheets for flexible and stretchable electronics, *Adv. Funct. Mater.*, 2019, **29**(37), 1902575.

8 Y. Yao, J. Sun, X. Zeng, *et al.*, Construction of 3d skeleton for polymer composites achieving a high thermal conductivity, *Small*, 2018, **14**(13), 1704044.

9 X. Zhang, J. Zhang, L. Xia, *et al.*, Simple and consecutive melt extrusion method to fabricate thermally conductive composites with highly oriented boron nitrides, *ACS Appl. Mater. Interfaces*, 2017, **9**(27), 22977-22984.

10 J. Zhang, X. Wang, C. Yu, *et al.*, A facile method to prepare flexible boron nitride/poly(vinyl alcohol) composites with enhanced thermal conductivity, *Compos. Sci. Technol.*, 2017, **149**, 41-47.

11 J. Ma, N. Luo, Z. Xie, *et al.*, Preparation of modified hexagonal boron nitride by ball-milling and enhanced thermal conductivity of epoxy resin, *Mater. Res. Express*, 2019, **6**(10), 1050d1058.

12 C. P. Feng, L. Bai, R. Y. Bao, *et al.*, Electrically insulating poe/bn elastomeric composites with high through-plane thermal conductivity fabricated by two-roll milling and hot compression, *Adv. Compos. Hybrid Mater.*, 2018, **1**(1), 160-167.

13 Y. Xue, X. Li, H. Wang, *et al.*, Improvement in thermal conductivity of through-plane aligned boron nitride/silicone rubber composites, *Mater. Des.*, 2019, **165**, 107580.

14 Q. Hu, X. Bai, C. Zhang, *et al.*, Oriented bn/silicone rubber composite thermal interface materials with high out-of-plane thermal conductivity and flexibility, *Compos. Part A Appl. Sci. Manuf.*, 2022, **152**, 106681.

15 T. Huang, Y. Li, M. Chen, *et al.*, Bi-directional high thermal conductive epoxy composites with radially aligned boron nitride nanosheets lamellae, *Compos. Sci. Technol.*, 2020, **198**, 108322.

16 J. Shi, W. Aftab, Z. Liang, *et al.*, Tuning the flexibility and thermal storage capacity of solid–solid phase change materials towards wearable applications, *J. Mater. Chem. A*, 2020, **8**(38), 20133-20140.

17 S. Gong, X. Li, M. Sheng, *et al.*, High thermal conductivity and mechanical

strength phase change composite with double supporting skeletons for industrial waste heat recovery, *ACS Appl. Mater. Interfaces*, 2021, **13**(39), 47174-47184.
18 W. Yang, R. Lin, X. Li, *et al.*, High thermal conductive and anti-leakage composite phase change material with halloysite nanotube for battery thermal management system, *J. Energy Storage*, 2023, **66**, 107372.
19 W. Zhang, X. Zhang, Y. Xu, *et al.*, Flexible polyethylene glycol/polyvinylpyrrolidone composite phase change fibres: Preparation, characterization, and thermal conductivity enhancement, *Polymer*, 2021, **214**, 123258.
20 Y. Lu, R. Hu, X. Chen, *et al.*, A strategy for constructing 3d ordered boron nitride aerogels-based thermally conductive phase change composites for battery thermal management, *J Mater Sci Technol*, 2023, **160**, 248-257.
21 J. Yang, L. S. Tang, R. Y. Bao, *et al.*, Largely enhanced thermal conductivity of poly (ethylene glycol)/boron nitride composite phase change materials for solar-thermal-electric energy conversion and storage with very low content of graphene nanoplatelets, *Chem. Eng. J.*, 2017, **315**, 481-490.
22 L. S. Tang, Y. C. Zhou, L. Zhou, *et al.*, Double-layered and shape-stabilized phase change materials with enhanced thermal conduction and reversible thermochromism for solar thermoelectric power generation, *Chem. Eng. J.*, 2022, **430**(2), 132773.
23 J. Yang, P. Yu, L. S. Tang, *et al.*, Hierarchically interconnected porous scaffolds for phase change materials with improved thermal conductivity and efficient solar-to-electric energy conversion, *Nanoscale*, 2017, **9**(45), 17704-17709.
24 Y. Wang, Y. Chen, W. Dai, *et al.*, Anisotropic black phosphorene structural modulation for thermal storage and solar-thermal conversion, *Small*, **19**(52), 2303933.